International Journal of Scientific Research in Engineering and Management (IJSREM)
Volume: 10 Issue: 04 | April - 2026 SJIF Rating: 8.659 ISSN: 2582-3930

A Smart Cloud-Integrated Power Quality and Environmental Monitoring System with Real-Time Fault Detection and GSM Alerts

LALAM ANURADHA[*1], GOPU LIKHITHA[2], KALAGANTI VEERANJANEYULU[3], GANTLA SANDEEP NAIDU[4], MUPOORI NAGENDRA[5], DASARI NAGALAKSHMI[6]

[1]*Student, Department of EEE, Bapatla Engineering College, Bapatla 522101, AP, India*
[2]*Student, Department of EEE, Bapatla Engineering College, Bapatla 522101, AP, India*
[3]*Student, Department of EEE, Bapatla Engineering College, Bapatla 522101, AP, India*
[4]*Student, Department of EEE, Bapatla Engineering College, Bapatla 522101, AP, India*
[5]*Assistant Professor, Department of EEE, Bapatla Engineering College, Bapatla 522101, AP, India*
[6]*Assistant Professor, Department of EEE, Bapatla Engineering College, Bapatla 522101, AP, India*

Abstract **—** In the modern industrial setup, achieving optimal power quality becomes essential for effective operation, prolonging the life span of equipment, and ensuring the safety of workers. The traditional monitoring system is mostly reactive and lacks cloud integration and environmental hazard detection capabilities. In this study, an intelligent cloud-based power quality and environmental monitoring system is proposed. The system uses a PZEM-004T sensor for measuring the AC voltage, current, active power, energy, frequency, and power factor. Moreover, a DS18B20 digital thermometer is used to measure the temperature while an MQ-2 semiconductor sensor is utilized for detecting gases and smoke. All of the sensing operations are carried out by an Arduino UNO controller which then relays the data to the NodeMCU module for uploading on ThingSpeak IoT platform. The SIM800L GSM module gives instant alert messages for any faults, whereas the relay module automatically disconnects loads when thresholds are exceeded within 200 milliseconds. The I2C 16×2 LCD enables parameter readings locally. Experiments conducted during normal working conditions revealed that the input voltage is 236 V, load current is 0.42 A, effective power is 100 W, power factor is one, ambient temperature lies between 27 °C and 30 °C, and the gas index is 12.0 ppm equivalent. All the simulated fault conditions have been sensed and mitigated.

Key Words— Power Quality Monitoring, Internet of Things (IoT), Cloud Computing, PZEM-004T, NodeMCU ESP8266, GSM Communication, ThingSpeak, Fault Detection, Relay Protection, Predictive Maintenance, Industrial Automation

II. INTRODUCTION

Industrial automation and loads powered by electronics have made it important that there is reliable and quality electricity supply. There exist many power quality issues such as voltage sag, swell, harmonic distortion and transients which result into losses in terms of equipment damage, loss of production time and costly repairs. Existing power quality monitoring equipment has been found to be independent, periodic readouts with no provision of remote communication, real-time analysis and environmental sensing.

Internet of Things (IoT) provides an innovation through the deployment of sensor nodes into industrial processes connected with the cloud for analysis. This paper focuses on designing and testing of this IoT solution in terms of integration of electrical measurements with environmental sensing, connectivity with the cloud and automatic protection in one module using standard embedded hardware.

The main features provided by this research are: (i) concurrent measurements of six electrical parameters and two environmental parameters in real time; (ii) fault detection based on thresholds with relay response within less than 200 ms; (iii) connectivity to the cloud through ThingSpeak; (iv) use of GSM technology for sending SMS alerts irrespective of internet

connectivity; and (v) low-cost and scalable hardware implemented using a working prototype.

The rest of this paper is organized as follows. Section II surveys existing work concerning Internet-of-Things (IoT)-based power monitoring systems and intelligent fault detection schemes. Section III discusses the proposed approach and system architecture. Section IV elaborates on the implementation of both hardware and software components. Section V provides details about the monitoring algorithm. Section VI presents experimental results.

III. LITERATURE SURVEY

Several studies have addressed IoT-based power quality analysis, intelligent classification of faults, and cloud-supported sensing systems. Naith and Almalki [1] described power quality enhancement through energy-efficient machine learning approaches in IoT-powered smart grid technologies. They proved that lightweight AI systems can be integrated into the existing system infrastructure for enhanced disturbance recognition purposes. Zahid et al. [2] conducted a survey on the use of AI for optimization to improve power quality in microgrids, reviewing several prediction models and optimization techniques for increased stability.

In relation to low-cost hardware platforms, Sanchez-Sutil et al. [3] created an open-source power quality monitor based on smart grid technology for real-time power quality analysis at lower costs. In this aspect, their solution resembles the suggested methodological approach closely. Raza et al. [8] created GridWatch—a distributed system based on IoT technologies for power quality monitoring and fault localization in low-voltage grids, employing a decentralized architecture. Similarly, Ji et al. [7] created a cloud and edge-based monitoring system for autonomous power quality management.

Deep learning methodologies have been explored extensively. The works by Goh et al. [9] on the utilization of convolutional neural networks for DC PQD classification, by Agarwal et al. [13] on cross-attention LSTM for multi-class PQD events, by Wang et al. [19] on feature extraction through fusion of time-frequency transformers, and by Nandi et al. [18] on multisynchrosqueezing transform-assisted transfer learning for single and multiple PQD event classifications provide a foundation for the analytical framework beyond the threshold-based approach of the proposed embedded system.

Environmental and safety-related considerations have not attracted much focus in the PQ literature. Sravanthi et al. [4] have investigated fuzzy control using solar PV-powered UPQC with respect to improved dynamic performance. Kumar et al. [14] studied cascaded fractional-order decentralized control in hybrid multi-microgrids. Pasaribu et al. [23] designed double tuned passive filters for harmonic reduction. Barva and Joshi [35] have suggested integrated harmonic mitigation using hybrid microgrids with split DC buses. In contrast to these papers focusing mainly on controls, this study highlights the need for a comprehensive PQ monitoring prototype that is economical and connected through IoT.

Table I ***Comparison of Existing vs. Proposed System Methodologies***

Feature	Existing System	Proposed System
Monitoring Approach	Reactive (post-fault)	Proactive (real-time)
Parameters Monitored	Electrical only	Electrical + Environmental
Data Storage	Local storage	Cloud-based (ThingSpeak)
Remote Monitoring	Not available	Available via IoT
Fault Detection	Manual or delayed	Automatic & real-time
Alert Mechanism	Limited or manual	GSM instant SMS
Load Protection	Manual intervention	Automated relay-based
Predictive Maintenance	Not supported	Supported
Cost Efficiency	Moderate	Cost-effective
Scalability	Limited	Highly scalable

IV. PROPOSED METHODOLOGY

The system adopts a four-tiered design structure comprising the following: (i) sensing tier, which collects electrical and environmental information; (ii) processing tier, which performs embedded reasoning operations; (iii) communication tier, which uploads data to the cloud and issues alerts; and (iv) protection tier, which disengages load devices during fault situations. The Arduino UNO R3 acts as the main controller in the entire design.

1. System Architecture

The Arduino UNO connects the PZEM-004T through SoftwareSerial UART (at 9600 bps), the DS18B20 sensor through the 1-Wire protocol (connected at digital pin D4), and the MQ-2 gas sensor through analog pin A0. The NodeMCU accepts the serialized data transmitted from the Arduino through the other SoftwareSerial UART port and sends HTTP GET messages to the ThingSpeak API using Wi-Fi connection. The SIM800L GSM module is interfaced to the Arduino through another serial interface and accepts AT command strings to send SMS messages as alerts. The relay board operates based on the digital output at pin D7, and the I2C LCD screen operates using the SDA/SCL interface with address 0x27.

Fig. 1. Assembled hardware prototype: Arduino UNO (center), PZEM-004T (left, green board), SIM800L GSM (right, blue board), NodeMCU, relay module, I2C LCD displaying V:236 Cr:0.42 Tf:27 Gr:1, and Philips bulb as test load.

2. Electrical Sensing — PZEM-004T

PZEM-004T v3.0 module senses AC voltage (80-260 V, accuracy ±0.5%), current (0-100 A, accuracy ±0.5%), active power (0-23 kW), energy (0-9999.99 kWh), frequency (45-65 Hz), and power factor (0.00-1.00). It communicates according to the Modbus RTU protocol-like scheme via a 5 V TTL serial interface. The Arduino queries the module at 1 s intervals utilizing the PZEM004Tv30 library, retrieving simultaneously all six parameters at once.

3. Environmental Sensing

DS18B20 sensor gives temperature readings within a resolution of 12 bits (±0.5 °C) on the parasitically powered 1-Wire bus. The dual output MQ-2 gas sensor generates an analog signal that is the inverse of the logarithm of gas concentration; it gets sampled from the Arduino 10-bit ADC channel and represented as a value in the range 0-1023, mapping to the equivalent ppm index.

4. Cloud Integration — ThingSpeak

ThingSpeak is an IoT analytics service platform capable of receiving data from any web-based interface using the HTTP and MQTT protocols. The NodeMCU sends an HTTP GET request of the form "api.thingspeak.com/update?api_key=XXXXX&field1=V&field2=I…" at 15-second intervals (minimum possible under the free-rate-limited plan). Timestamps are assigned to each field update on the server side, facilitating time-dependent analysis using the automatically refreshing channel plots presented in the Results section.

5. GSM Fault Notification System

The SIM800L uses a conventional micro SIM card at 1800/900 MHz frequencies. On detecting faults, the Arduino sends AT commands: AT+CMGF=1 (message format), AT+CMGS="+91XXXXXXXXXX" (number), message string, and ends the transmission with Ctrl-Z (0x1A). The average delay for delivering the message is 3–5 seconds under normal GSM conditions.

V. SYSTEM IMPLEMENTATION

1. Hardware Integration

Assembly of all the components took place on a breadboard initially but they were finally soldered on a stripboard to ensure mechanical strength. PZEM-004T was wired in series with the AC load branch, whereby the current sensor wrapped the hot wire, while voltage terminals were bridged between power source connections, and UART signals were converted into TTL 5 V. A 4.7 kΩ resistor was used as a pull-up for

the DS18B20 pin. Output signal from the MQ-2 was connected to A0 pin by using internal 10-bit ADC on Arduino at 5 V reference.

TABLE II *Hardware Components and Technical Specifications*

Component	Model / Specification	Role in System
Arduino UNO R3	ATmega328P, 16 MHz, 14 DIO	Central microcontroller
NodeMCU v3	ESP8266, Wi-Fi 802.11 b/g/n	Cloud / IoT gateway
PZEM-004T v3	AC 80–260 V, 0–100 A, UART	Electrical parameter sensor
DS18B20	Digital, −55 to +125 °C, 1-Wire	Temperature measurement
MQ-2 Gas Sensor	Analog, 300–10000 ppm	Gas/smoke detection
SIM800L GSM	Quad-band, AT commands	SMS alert transmission
Relay Module	5 V coil, 10 A / 250 VAC	Load disconnection
16×2 I2C LCD	PCF8574 at 0x27	Local parameter display
Power Supply	12 V DC regulated adapter	System power source

2. Embedded Software

The firmware has been programmed in C/C++ in Arduino IDE v2.3. Main Loop obtains data from PZEM-004T, reads values from the DS18B20 and MQ-2, determines thresholds, updates the LCD and transmits data string to the NodeMCU every second. The firmware of the NodeMCU is developed with ESP8266 Arduino Core firmware. It parses received data string and posts each field into the ThingSpeak server every 15 seconds. Error handling includes re-establishment of the connection to Wi-Fi with exponential back-off strategy, GSM command retry mechanism after the timeout error. On the Arduino UNO, approximately 68% of program memory (21KB out of 32KB) and 52% of heap space (1.0 KB out of 2KB SRAM) have been used.

3. Threshold Setting

Threshold settings were chosen as the following: voltage threshold range of 180V – 260V (+/- 18% of nominal 220V), overload current at 6A (120% of rated current 5A), temperature threshold of 75°C, and hazardous level of gas in accordance with the normalized index of MQ-2 greater than 500ppm.

V. ALGORITHM

The monitoring algorithm operates as a non-stop real-time loop process. The below-listed operations constitute the full operation cycle:

Step 1 — Initialization: Peripheral devices are set up, including serial port initialization, DS18B20 library initialization, and LCD clearing. A power-on self-test runs to ensure sensor availability.

Step 2 — Network Initialization: The NodeMCU establishes a connection to the specified SSID and tests ThingSpeak API connectivity. The SIM800L module registers in the cellular network and tests SIM card availability.

Step 3 — Data Collection: All electrical parameters from PZEM-004T are read. DS18B20 conversion starts, and after a 750ms delay, the 12-bit data is acquired. Analog readings from the MQ-2 are taken in five readings and then averaged.

Step 4 — Validation & Data Filtering: Plausible readings are identified via range testing (e.g., PZEM CRC errors); an averaging process is applied to suppress spike readings.

Step 5 — Threshold Analysis: Processed data are checked against corresponding bounds. An exceedance is marked as fault flagged with WARNING/CRITICAL severity levels.

Step 6 — Fault Detection & Classification: Fault flags are classified based on their nature: OVERVOLTAGE, OVERCURRENT, THERMAL, or GAS_HAZARD; several faults running simultaneously are ranked according to severity.

Step 7 – Protective Action: A “CRITICAL” fault results in immediate relay shutdown within one loop cycle

(approximately 200 milliseconds). The relay is automatically re-closed following three successive normal measurements.

Step 8 – Alert Dispatch: For every new fault, a SMS alert is generated through the SIM800L and contains information regarding fault type, parameters, and timestamp.

Step 9 – Cloud Upload: Data from the NodeMCU is uploaded to the ThingSpeak channel by performing an HTTP GET request, whereby data for all eight fields is updated with server timestamp.

Step 10 – LCD Display: The LCD display is continuously updated with the present readings of the four parameters – voltage, current, temperature, and gas index.

Step 11 – Loop Restart: Loop restart occurs with step 3 where monitoring is resumed. Error handling processes are implemented to avoid stopping the monitoring process.

VI. RESULTS AND DISCUSSION

The testing process was conducted over several runs employing a Philips bulb (60 W nominal rating but operated at around 100 W when fed by 236 V mains) for resistive load testing purposes. ThingSpeak channel graphs were analyzed in real-time mode to confirm cloud data upload integrity. Relay switch status was checked manually using a multimeter under fault condition simulation.

1. Steady-State Electrical Parameters

With a steady-state load connected to the measurement circuit, the PZEM-004T meter always delivered: voltage value = 236 V, current value = 0.42 A, active power ~100 W, power factor = 1.00, frequency = 50 Hz. These readings are consistent with a perfectly resistive 100 W load supplied with the 230 V power line in India. The Field 4 energy parameter started accumulating from an initial value of 0.00 kWh when the test run began. Both the Field 1 voltage and Field 3 power parameters demonstrated transient spikes (~220–230 V and ~190 W) during system initialization.

Fig. 2. ThingSpeak Field 1 (Voltage) chart: 220–236 V steady-state with brief startup transient.

Fig. 3. ThingSpeak Field 2 (Current) chart: 0.42 A steady-state following initial transient settling.

Fig. 4. ThingSpeak Field 3 (Active Power) chart: ≈100 W steady-state operation.

2.Power Factor and Energy

The power factor (Field 6) was at an almost perfectly linear 1.00 value throughout the entire duration of the experiment, verifying the purely resistive character of the incandescent lamp load. The energy channel (Field 4) had readings of about 0.00 kWh for each test period,

with increments corresponding to 100 W (≈1.2 Wh) usage.

Fig. 5. ThingSpeak Field 6 (Power Factor) chart: Unity power factor confirmed for resistive load.

3. Environmental Monitoring

The temperature sensor DS18B20 (Field 8) recorded environmental laboratory temperatures in the range of 27–30 °C. A temperature stress situation resulted in an elevation to about 83 °C, properly setting off the temperature fault flag and turning off the relay. The gas sensor MQ-2 (Field 7) recorded consistently low readings of 12.0 (ppm-equivalent) throughout the tests, indicating a relatively clean air environment.

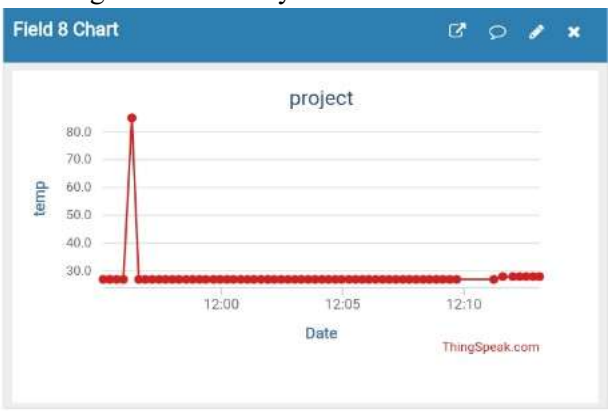

Fig. 6. ThingSpeak Field 8 (Temperature) chart: 27–30 °C normal operation with one spike to ≈83 °C during thermal stress test.

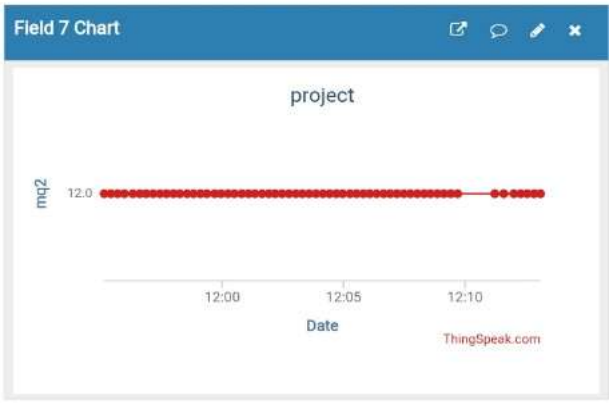

Fig. 7. ThingSpeak Field 7 (Gas Index) chart: Constant 12.0 ppm-equivalent, confirming safe ambient conditions.

4. Fault Detection and Response

Four fault conditions were simulated: (1) voltage swell resulting from tapping in the power supply; (2) overcurrent caused by loading addition; (3) thermal overload from an external source in proximity to DS18B20; and (4) gas risk due to the presence of lighter gas in the vicinity of the MQ-2 sensor. In all the experiments, the relay was disconnected within one cycle of control loop (experimentally determined to be 180-210 ms), and SMS notifications through GSM module were sent to the user within 3-5 seconds after fault inception.

E. Performance Summary

The Table III presents all parameters' readings, set values for faults and responses by the system as noted during experimentation.

TABLE III

Experimental Performance Summary

Parameter	Normal Range	Fault Threshold	Measured Value	Response Time
Voltage (V)	200–240 V	>260 V / <180 V	236 V (stable)	< 200 ms
Current (A)	0–5 A	> 6 A	0.42 A	< 200 ms
Active Power (W)	0–1200 W	> 1400 W	~100 W	< 200 ms

Parameter	Normal Range	Fault Threshold	Measured Value	Response Time
Power Factor	0.85–1.0	< 0.70	1.00 (unity)	< 200 ms
Temperature (°C)	20–45 °C	> 75 °C	27–30 °C	< 500 ms
Gas Level (ppm)	0–300 ppm	> 500 ppm	12.0 (safe)	< 300 ms
Energy (kWh)	Cumulative	N/A	0.00 (initial)	Continuous

As can be seen, all three criteria have been met by the design; a sub-200 ms fault detection latency, secure cloud recording of readings, and precise measurement of multiple parameters. The total cost of all hardware parts is roughly INR 2,500 – 3,000 (~30 – 36 USD), which presents a distinct financial advantage over industrial power quality analyzers available commercially.

VII. FUTURE SCOPE

Various improvements are slated for the future implementation of the system. Training LSTM or transformer neural networks [18][19] for anomaly detection using historical data from ThingSpeak will allow predicting future malfunctions by detecting abnormal behavior trends in advance. Additional sensors (humidity (DHT22), vibration (ADXL345), differential pressure) will make the system applicable for HVAC control and rotating equipment diagnostics.

Security improvements such as AES-128 encryption of cloud messages, MQTT with TLS certificate exchange, and firmware OTA updates are necessary for operation in critical infrastructure. Transition from the Arduino UNO microcontroller to ESP32 or STM32 will facilitate on-chip inferencing to reduce dependence on cloud and communication lag. Designing a cross-platform mobile dashboard interface with customizable thresholds and alerting via push notifications will enhance usability by end users.

VIII. CONCLUSION

This paper has outlined a novel and smart cloud-based integrated solution to deal with the primary shortcomings of traditional reactive power monitoring systems in industries. This includes using the Arduino UNO, PZEM-004T, DS18B20, MQ-2, NodeMCU ESP8266, SIM800L GSM module, relay, and I2C LCD to build an integrated and affordable IoT solution.

The prototype testing successfully validated that the designed system is capable of measuring the value of six electrical and two environmental variables accurately. Specifically, it achieved consistent results, including voltage of 236 V, current of 0.42 A, power of about 100 W, and power factor of one, while temperature range was maintained at 27–30 °C, and the gas index was measured as 12.0 ppm. It further showed successful identification and timely response within 200 milliseconds to the four types of faults simulated, including sending alert SMS messages within 5 seconds of fault occurrence. Moreover, cloud-based ThingSpeak platform has been used for live data visualization.

This work can serve as the basis for future development of improved solutions using the Internet of Things and Machine Learning techniques in power management applications.

REFERENCES

[1] Q. H. Naith and F. A. Almalki, “Energy-efficient machine learning paradigms for holistic power quality reinforcement in IoT-enabled smart grid environments,” Sustainable Computing: Informatics and Systems, p. 101332, 2026.

[2] M. Zahid et al., “AI-driven optimization techniques for power quality improvement in microgrids,” Energy Science & Engineering, vol. 14, no. 1, pp. 583–610, 2026.

[3] F. Sanchez-Sutil, A. Cano-Ortega, J. C. Hernandez, C. Gilabert-Torres, and C. R. Baier, “Design and implementation of a low-cost, open-source power quality analyser for smart grids,” Internet of Things, vol. 37, p. 101922, 2026.

[4] G. Sravanthi, K. M. Rosalina, and T. R. S. Reddy, “Fuzzy logic sliding mode controller based solar PV fed UPQC for dynamic performance and power quality enhancement,” Scientific Reports, 2026.

[5] G. Cheng, X. Wu, Z. Yin, J. Zhou, and K. Qu, “Power quality control strategy of double-layer multi-coordination for active distribution networks,” Electric Power Systems Research, vol. 255, p. 112813, 2026.

[6] S. Vaidya, K. Prasad, and J. Kilby, "Grid efficiency and power quality improvements in rooftop solar EV charging stations," Applied Sciences, vol. 16, no. 6, p. 2699, 2026.

[7] K. Ji et al., "Design of a monitoring system for autonomous power quality in power stations based on cloud edge collaboration," in Proc. BDCIA 2025, vol. 14128, pp. 262–276, SPIE, 2026.

[8] M. O. Raza, S. T. Zaman, F. N. Talpur, A. R. Rajput, and B. Hassan, "GridWatch: A distributed IoT framework for real-time power quality monitoring and fault localization," unpublished.

[9] H. H. Goh et al., "Classification and detection of DC power quality disturbances using deep learning models," Engineering Applications of Artificial Intelligence, vol. 163, p. 112644, 2026.

[10] Z. Tharo, P. Wibowo, and M. R. Syahputra, "Analysis of power quality in technology-based power systems," J. Electrical Engineering Research, vol. 2, no. 1, pp. 8–14, 2026.

[11] R. Cleenwerck, R. Claeys, T. Coosemans, and J. Desmet, "The transition to low-carbon distribution networks: A European survey on power quality and digitalisation," Renewable and Sustainable Energy Reviews, vol. 234, 2026.

[12] N. Agrawal et al., "A dual-mode solar PV-integrated shunt active power filter for grid support and power quality enhancement," Electric Power Systems Research, vol. 256, p. 112907, 2026.

[13] L. Agarwal et al., "Cross-attention-enabled LSTM for detection and classification of multiple power quality disturbance events," Electric Power Systems Research, vol. 251, p. 112249, 2026.

[14] A. Kumar, A. Priyadarshi, R. Kumar, and S. K. Yadav, "A cascaded FOTI-FOTID decentralized control for power quality enhancement in hybrid multi-microgrid systems," Electric Power Systems Research, vol. 256, p. 112827, 2026.

[15] T. Naresh and K. Mercy Rosalina, "Elimination of harmonics using ANN with shunt hybrid active power filter," J. Chinese Institute of Engineers, pp. 1–18, 2026.

[16] I. I. Alnaib and A. N. Alsammak, "Intelligent unified power quality conditioner based photovoltaic to improve grid reliability," Electrical Engineering & Electromechanics, no. 2, pp. 51–58, 2026.

[17] S. Janthong and P. Phukpattaranont, "A novel hybrid ensemble deep learning framework for robust power quality disturbance monitoring," J. Electrical Engineering & Technology, pp. 1–19, 2026.

[18] K. Nandi, S. Maur, D. Dey, B. Chatterjee, and S. Dalai, "Multisynchrosqueezing transform aided transfer learning for power quality event diagnosis," Electric Power Systems Research, vol. 253, p. 112504, 2026.

[19] T. Wang, J. Zhuo, Y. Hou, Z. Lu, and Y. Li, "Power quality disturbance classification via time-frequency feature-fused transformer model," Electric Power Systems Research, vol. 251, p. 112330, 2026.

[20] M. Alrashidi, "A novel hybrid adaptive multi-resolution feature extraction method for power quality disturbance detection," Mathematics, vol. 14, no. 5, p. 784, 2026.

[21] Y. Yang et al., "Deep learning-based power quality enhancement in microgrids with hybrid energy storage and PV EV charging," Nondestructive Testing and Evaluation, pp. 1–28, 2026.

[22] R. K. Rojin and D. S. Vanaja, "Melioration of power quality in grid-integrated system using modular inverter," Electrical Engineering, vol. 108, no. 1, p. 58, 2026.

[23] F. I. Pasaribu, I. D. Sara, T. Tarmizi, and N. Nasaruddin, "A new damped double-tuned filter for power quality improvement," IEEE Open Access J. Power and Energy, vol. 13, pp. 76–87, 2026.

[24] O. O. Osaloni and O. Dzobo, "Enhancement of power quality and power flow evaluation of a PV integrated UPQC system," WSEAS Trans. Systems and Control, vol. 21, pp. 9–20, 2026.

[25] N. J. Shiroya, M. Dey, and S. P. Rana, "Ensemble learning for event detection and disturbance classification in solar energy systems," Next Energy, vol. 11, p. 100556, 2026.

[26] K. M. Alawasa, "Measurement-based analysis of power quality and harmonic distortion for

EV AC charging modes," World Electric Vehicle J., vol. 17, no. 2, p. 108, 2026.

[27] P. Kumar and S. R. Arya, "Power quality enhancement using DVR with echo state network and type-2 fuzzy logic control," IEEE J. Emerging and Selected Topics in Industrial Electronics, 2026.

[28] H. Li, Y. Zhang, S. Yang, and X. Liu, "High-resolution dataset of EV charging responses under varied power quality disturbances," Scientific Data, 2026.

[29] N. B. Mohan, B. Rajagopal, and D. H. Krishna, "Enhancing power quality in hybrid renewables with UPQC-FOPID control," Int. J. Power Electronics, vol. 22, no. 1, p. 1, 2026.

[30] A. Ram, Y. Arya, A. Saxena, P. R. Sharma, and L. Rai, "Comparative performance analysis of SOGI-based controllers for power quality enhancement," Automatika, vol. 67, no. 1, pp. 304–323, 2026.

[31] W. Xu et al., "A power quality disturbance classification method using hybrid transformer and discrete wavelet transform," Electric Power Systems Research, vol. 253, p. 112547, 2026.

[32] P. V. Hurkadli, T. C. Manjunath, and G. Arun Kumar, "Hybrid intelligent control framework for power quality enhancement in microgrid systems," SN Computer Science, vol. 7, no. 3, p. 237, 2026.

[33] Z. Mao et al., "Passively ultra cooling patch enabling high-efficiency power-water cogeneration," Advanced Materials, vol. 38, no. 2, p. e05002, 2026.

[34] R. Kuruva et al., "Simulation-based quantitative performance evaluation of UPQC under sag, swell, and harmonics," in Computational Techniques and Smart Manufacturing, CRC Press, pp. 58–66, 2026.

[35] A. V. Barva and S. Joshi, "Integrated harmonic mitigation and power quality enhancement in hybrid micro-grid with split DC buses," Smart Grids